Refolding Behavior of a Kinetic Intermediate Observed in the Low pH Unfolding of Ribonuclease A†

Paul J. Hagerman,‡ Franz X. Schmid,§ and Robert L. Baldwin*

ABSTRACT: A transient intermediate (I_3) observed previously in the unfolding of ribonuclease A has been studied by employing a sequential mixing instrument to populate selectively this species. This approach has made it possible both to determine the refolding behavior of this species and to characterize further the kinetics of its formation. (1) Formation of I_3 represents the earliest detectable change in unfolding. (2) The loss of the 2′CMP binding site occurs in parallel with the exposure of the interior of the protein to solvent. (3) I_3 is distinct from previously described intermediates in refolding. (4) Overall condensation of the protein to exclude solvent from the interior, as well as the formation of a substrate binding site, takes place in approximately 30 ms (pH 5.8, 47 °C), indicating that the formation of native structure can take place faster than had previously been supposed.

In a previous study of the pH-induced unfolding[1] of RNase A,[2] the linear three-species model

$$U_1 \underset{\text{slow}}{\rightleftharpoons} U_2 \underset{\text{fast}}{\rightleftharpoons} N$$

proposed by Garel & Baldwin (1973, 1975a,b) was extended to include an additional intermediate in unfolding (I_3)

$$U_1 \rightleftharpoons U_2 \rightleftharpoons I_3 \rightleftharpoons N$$

based on the observation of triphasic kinetics in pH jumps ending above the final T_m. In both models, U_1 and U_2 represent relatively unfolded species present in and above the transition zone, and N (native enzyme) is present in and below the transition zone. The assignment of I_3 was based on the appearance above the final T_m of a relatively unfolded intermediate prior to the formation of U_1 and U_2. Several additional features of this rapidly formed species are known (Hagerman & Baldwin, 1976), namely: (1) I_3 represents less than 2% of the species present in solution at equilibrium throughout the transition zone; (2) the equilibrium ratio (I_3/U_2) varies by less than a factor of two over a temperature range where I_3/N changes by over 1000; and (3) the molar absorbance at 287 nm of I_3, which measures the exposure of tyrosine groups to solvent, is quite similar to those of U_1 and U_2.

More recent evidence from pH- and Gdn·HCl-induced folding of RNase A (Nall et al., 1978), temperature-jump, NMR studies (Blum et al., 1978), and kinetic studies of RNase A using ^3H exchange (Schmid & Baldwin, unpublished results) all indicate that partially folded intermediates (I_1 and I_2) are formed rapidly compared with the formation of N, suggesting a model of the form

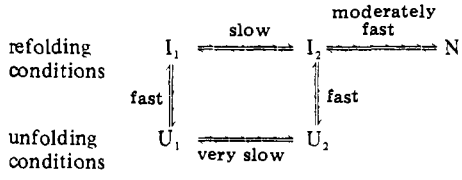

for refolding.

The previous characterization of I_3 does not allow its integration into the above model for folding, since the relationship between I_1 and I_2, and I_3 is not known. A more complex analysis of I_3, including a determination of its binding properties as well as identification of any additional intermediates, has not previously been possible because I_3 is never significantly populated at equilibrium.

In this paper, the existence of the transient intermediate (I_3) is directly verified and I_3 is shown to be distinct from I_1 and I_2, using a sequential mixing instrument (which produces two reactions in rapid succession) designed for the detection and characterization of transient intermediates. This experimental approach has the distinct advantage over conventional stopped-flow experiments in that large populations of transient intermediates are selectively produced (see below).

Experimental Section

Sequential-Jump Measurements. Such measurements involve two standard stopped-flow reactions in rapid succession, where the product of the first reaction constitutes one of the two reactants of the second reaction. The rationale for this approach is indicated in the legend to Figure 1.

Instrumental Design. The general instrumental layout for the sequential-mixing device is presented schematically in Figure 2. For details of construction and operation, see Hagerman (1977). The sequential-mixing instrument provides a time delay between the first and second mixing events, produced by solution flowing at a fixed velocity through a precisely defined length of tubing. This basic design principle is similar to that employed by Ballou (1971) and by McClure (personal communication), although extensive modifications have been made in order to accommodate optical detection. The current range of instrumental delays is from 5 ms to approximately 200 ms, depending on the delay line as well as the driving velocity employed.

Although the basic instrument is designed to measure absorbance changes, a minor modification of the observation chamber allows the detection of fluorescence changes. Moreover, the instrument can be employed for isotopic labeling experiments or a combination of labeling and optical detection.

† From the Department of Biochemistry, Stanford University Medical Center, Stanford, California 94305. *Received September 20, 1978.* Supported by research grants to Robert L. Baldwin from the National Science Foundation (PCM 77-16834) and the National Institutes of Health (2ROI GM 19988-18) and by a Medical Scientist Training Program Grant to Paul J. Hagerman from the National Institutes of Health (GM 1922). This article is taken in part from the Ph.D. Thesis of Paul J. Hagerman.

‡ Present address: Department of Chemistry, University of California at San Diego, La Jolla, California 92093.

§ Present address: FB Biologie, Universität Regensburg, 8400 Regensburg, West Germany.

[1] The term "protein folding/unfolding" is defined operationally as the reversible passage of a protein (S–S bonds intact) through the thermal transition zone.

[2] Abbreviations used: RNase A, bovine pancreatic ribonuclease A; T_m, temperature midpoint of the transition curve for thermal unfolding; τ, time constant of a reaction or kinetic phase (reciprocal of the apparent rate constant); α, a relative amplitude of a kinetic phase (fraction of the total amplitude); Gdn·HCl, guanidine hydrochloride; T-jump, temperature jump.

0006-2960/79/0418-0293$01.00/0

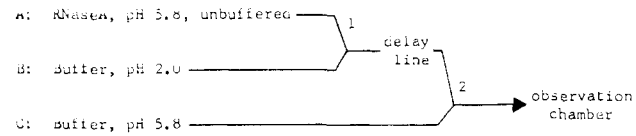

FIGURE 1: General mixing arrangement for a sequential-jump experiment, using the unfolding (pH 5.8 → 2.0)/refolding (pH 2.0 → 5.8) reactions of RNase A as an example. As solutions A and B are mixed, unfolding of RNase A begins and is reversed when the product of the first mixing event mixes with solution C. In the observation chamber a refolding process is taking place so that refolding rates are observed directly; however, the amplitude of the refolding process depends on how long unfolding was allowed to proceed, so information regarding the kinetics of unfolding can be obtained by plotting the amplitudes for the refolding process as a function of the delay time between 1 and 2.

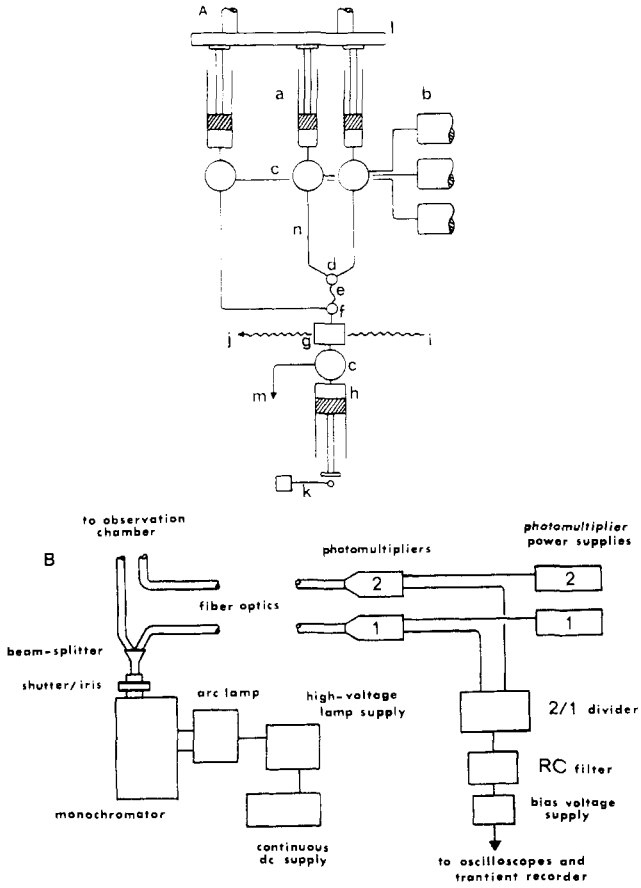

FIGURE 2: (A) Outline of the sequential-mixing instrument. For design details, see Hagerman (1977). (a) Hamilton, gas-tight driving syringes; (b) storage syringes; (c) three-way, high-pressure valves (Cheminert, Kel-F); pneumatically actuated, gang driven; (d) first stage mixing jet (Gibson-Milnes mixer); (e) calibrated delay line (high-pressure Teflon); for calibration procedure, see Experimental Section; (f) second stage mixing jet; (g) observation chamber—stainless steel chamber (0.159 cm diameter, 1.131 cm long) with quartz windows at each end to which are attached quartz fiber optics; (h) collection syringe (Hamilton, gas-tight); (i) light source (see B); (j) signal detection and processing (see B); (k) variable delay, data collection trigger; (l) driving assembly, cam follower, syringe driver; (m) purge for collection syringe; (n) high-pressure, precision bore Teflon tubing. Components a–g and n are all contained in an open, stainless-steel chamber through which water is circulated for temperature regulation. (B) Schematic outline of the signal generation and processing portions of the sequential-mixing instrument. The fiber optics are metal-clad quartz bundles that transmit light of wavelengths above 220 nm. These bundles are in turn polymer clad to seal against water. The beam splitter is a randomized division of one, 2000-fiber bundle into two, 1000-fiber bundles, one forming the reference channel (1) and the other forming the observation channel (2). This randomized division of fibers substantially reduces the noise caused by arc wander and intensity fluctuations.

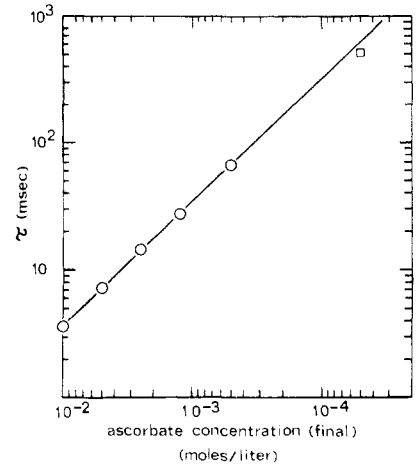

FIGURE 3: Log–log plot of the characteristic time for the reduction of DCIP by ascorbate, as a function of ascorbate concentration (see text for solution compositions), here represented by open circles. These data were obtained on a modified Durrum stopped-flow apparatus described elsewhere (Hagerman & Baldwin, 1976). The single datum represented by an open square was obtained on the sequential-mixing apparatus under conditions of slightly increased DCIP concentration and approaching conditions where ascorbate concentration is no longer in vast excess over DCIP concentrations.

Materials. (a) RNase A was from Worthington no. RAF 53N523 phosphate-free lyophilized powder, stored at −20 °C; concentration was determined by absorbance at 278 nm, neutral pH, using a molar absorbance of 9.8×10^3 (Sela & Anfinsen, 1957). (b) 2′CMP was P-L Biochemicals no. 273-10; concentration was measured using a molar absorbance of 7.6×10^3 at 260 nm, neutral pH (Beaven et al., 1955). (c) Other reagents were $NaClO_4$, Fisher Scientific; cacodylic acid, Fisher Scientific; sodium ascorbate, J. T. Baker; dichlorophenolindophenol (DCIP), Sigma. These reagents were used without further purification.

Solutions. (a) RNase A solutions were prepared by the general procedures for preparing and handling protein solutions as described elsewhere (Hagerman & Baldwin, 1976). All initial protein solutions are unbuffered. (b) Specific DCIP, ascorbate, and buffer solutions are described in the figure legends.

pH Measurements. pH values were all determined at 24 °C on a Corning Digital-110 pH meter using a Metrohm AG 9100 combined electrode.

Delay Line Calibration. A colorimetric reaction involving the reduction of DCIP by ascorbate provides a convenient means by which both mixing and delay times can be determined. As far as these authors are aware, the first use of this reaction for instrumental calibration was by K. Hiromi of Kyoto University (Tonomura et al., 1978). The reaction is followed at $\lambda = 517$ nm and, under conditions of ascorbate excess, is pseudo first order. The reaction rate varies linearly with ascorbate concentration over three orders of magnitude (Figure 3). Delay lines were calibrated by determining what portion of a standard DCIP reaction has occurred by the time the reactants enter the observation chamber.

Data Retrieval and Analysis. Oscilloscope traces were photographed with a Polaroid camera using type 107 black and white film. The photographs were digitized using the Hewlett-Packard 9864A digitizer and 9810A calculator and were then analyzed using least-squares, curve-fitting programs developed by Dr. A. Labhardt.

Results

A Rapidly Formed, Transient Intermediate in the Unfolding Pathway of RNase A Can Be Selectively Populated by a

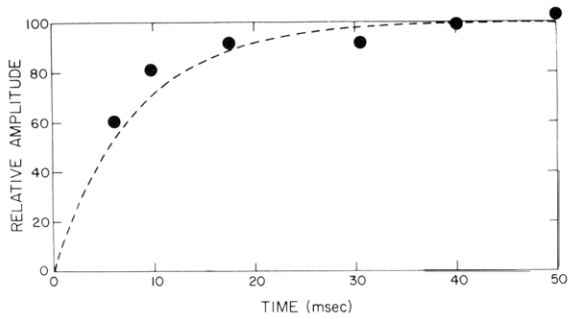

FIGURE 4: Comparison of the directly observed, rapid unfolding process τ_3 (Hagerman & Baldwin, 1976), measured at pH 2.0, 47 °C, with the same process as determined by the double-jump method, in which the relative amplitude of refolding is measured after brief periods (6–60 ms) of unfolding. (---) curve for τ_3 = 8 ms obtained from direct (pH 7.0 → 2.0) unfolding data. (●) Represent amplitudes (normalized) for refolding after various times of unfolding in the sequence pH 5.8 → 2.0 → 5.8. Absorbance is measured at λ = 287 nm. Initial conditions and conditions following the first mixing event, as well as conditions following the second mixing event, are given in the legend to Table II. Temperature = 47 °C.

Sequential Unfolding (pH 5.8 → 2.0)/Refolding (pH 2.0 → 5.8) Reaction Sequence. In the pH-induced unfolding of RNase A (pH 7.0 → 3.0), ending above the final T_m (43 °C, pH 3.0), triphasic kinetics are observed (Hagerman & Baldwin, 1976). The fastest process (designated τ_3 by those authors) occurs on a time scale of ~100 ms at T_m to ~10 ms at the upper end of the final transition zone. This process dominates the unfolding kinetics at the higher temperatures. The results suggest an unfolding model of the form

$$N \rightarrow I_3 \rightarrow U_2 \rightleftharpoons U_1$$

where N, I_3, and U_1 and U_2 are defined in the introductory section. In this scheme, I_3 is created rapidly compared with the conversion to U_2 and so accumulates at early times during unfolding.

The conditions used to populate I_3 are as follows. All experiments are performed at 47 °C and an unfolding pH of 2.0 because RNase A is almost completely unfolded at pH 2.0, 47 °C, and completely native at pH 5.8, 47 °C (Garel & Baldwin, 1973). pH 5.8 is chosen for refolding to optimize 2′CMP binding. In the unfolding experiment (pH 5.8 → 2.0, 47 °C), a value of τ_3 of 8 ± 4 ms is observed (Figure 4), both by direct kinetic measurements and by employing the double-jump method (described in Experimental Section). With this latter technique, the unfolding reaction (pH 5.8 → 2.0) occurs as the first of two processes, the second process being the reverse of the first: namely, the refolding reaction (pH 2.0 → 5.8). This second reaction can be initiated in a time range of 5–50 ms after the start of the first reaction, with the result that relatively slow-forming species such as U_1 and U_2 (defined earlier) are never populated. Under the conditions employed for these experiments, τ_2(unfolding) > 100 ms and τ_1(unfolding) > 1 s, so only the intermediate I_3 can be significantly populated within the 50-ms delay period.

By successively increasing the delay times from 5 to 50 ms, I_3 would become increasingly populated (Figure 4), and amplitudes associated with the subsequent refolding process ($I_3 \rightarrow N$) are expected to increase until the pseudo-equilibrium distribution between I_3 and N is achieved. As can be seen by inspection of Figure 4, the rise in amplitude, followed at 287 nm (burying of tyrosines), agrees reasonably well with the curve measured by direct unfolding. In Figure 5, an individual kinetic measurement is presented. The refolding results show only one kinetic phase, which indicates that no intermediates

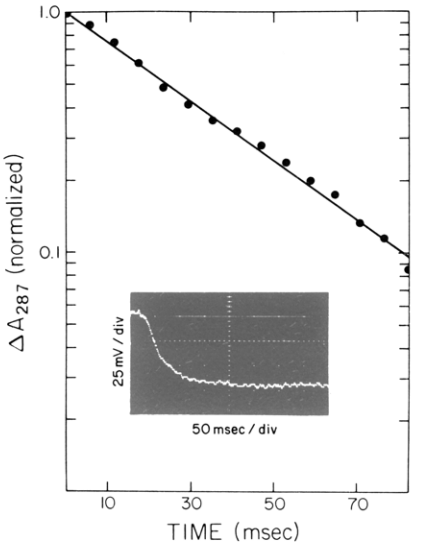

FIGURE 5: Oscilloscope recording (and normalized log plot) of refolding following a 50-ms period of unfolding. Initial unfolding (following first mixing event) and refolding (final conditions; following second mixing event) conditions are specified in the legends to Figure 4 and Table II. Refolding monitored by following the burying of tyrosines (A_{287}). The initial portion of the trace represents the period of time during which solution is flowing through the observation chamber.

Table I: Comparison of Amplitudes for Unfolding and Refolding[a]

expt	absorbance change (ΔA_{287})
sequential jump (refolding phase plateau)	0.021 ± 0.003 (expected: 0.023 ± 0.003)[b]
fastest process in total unfolding (τ_3)	−0.022 ± 0.003
total refolding	0.030 ± 0.003

[a] Comparison of the amplitudes associated with refolding, following a 50-ms period of unfolding, and total refolding. In both experiments, the refolding and unfolding conditions are identical (see legend to Table II). In the sequential jump experiment, the 50-ms delay was chosen to represent the plateau value for population of I_3 (see Figure 4). The total refolding experiment refers to refolding to pH 5.8 from protein solution preequilibrated at pH 2.0. Both experiments were performed at 47 °C with λ = 287 nm. Final solutions in both experiments were identical: 1.0 mg/mL of RNase A, 0.10 N $NaClO_4$, 0.10 N sodium cacodylate, pH 5.8. [b] The ΔA_{287} values observed for sequential refolding and the rapid phase of total unfolding are expected to be only 70–80% of the overall unfolding (or refolding) amplitude since, for unfolding to pH 2.0 at 47 °C (13 °C above T_m at pH 2.0), only that fraction of the unfolding process occurs in the millisecond time scale (Tsong et al., 1972). This same figure (70–80%) is predicted from the data of Hagerman & Baldwin (1976), who observed that the rapid reaction (population of I_3) comprised ~80% of the overall unfolding process 13 °C above T_m (at pH 3.0).

are populated in the folding of I_3 to N, when folding is monitored by tyrosine absorbance. The same result is obtained when formation of N is detected by binding of the specific inhibitor 2′CMP.

The Predominant RNase A Species in Solution during the First 50 ms Following the Start of Unfolding Is I_3. The change in absorbance (ΔA_{287}) for a refolding jump following a 50-ms period of unfolding is 70% of the change observed for complete refolding (single jump; Table I). Nall (1976) demonstrated that in unfolding experiments ending well above the final transition zone (pH 6.0, no Gdn·HCl → pH 2.1; [Gdn·HCl] up to 5.0 M; T = 45 °C) the fast process (τ_3) accounted for up to 97% of the entire optical change (λ = 287 nm). Without adding a denaturant such as Gdn·HCl, it has not been possible to obtain the entire optical change in the fast

Table II: Time Constants of the Refolding Reactions[a]

expt	obsd kinetics	time constants
single jump, refolding (pH 2.0 → 5.8; 47 °C)	biphasic	
	slow phase (τ_1)	10 ± 1 s
	fast phase (τ_2)	200 ± 20 ms
double jump, refolding	monophasic	29 ± 5 ms
		30 ± 5 ms[b]

[a] Comparison of the kinetics of complete refolding with those for refolding following a brief period (50 ms) of unfolding. The unfolding and refolding conditions are identical in both experiments. The final conditions are as follows: for unfolding, 0.1 N $NaClO_4$, adjusted to produce a final pH 2.0 ± 0.05 with $HClO_4$, unbuffered; for refolding, 0.1 N $NaClO_4$, adjusted to produce a final pH 5.8 ± 0.05 with $HClO_4$/NaOH; 0.05 M sodium cacodylate, final buffer concentration. Initial protein solutions were unbuffered. Final protein concentrations were ≅1 mg/mL in all experiments. Absorbance changes were monitored at λ = 287 nm (burying of tyrosines) except as noted. [b] Binding of 2′CMP to native RNase A was monitored at λ = 250 nm, where there is very little change in protein absorbance upon refolding (final 2′CMP concentration, 10^{-4} M; Garel & Baldwin, 1973). Under these conditions, 2′CMP binding to native RNase A takes place in less than 3 ms (Hammes, 1968; Garel & Baldwin, 1973).

unfolding reaction (Tsong et al., 1972; Hagerman & Baldwin, 1976). Consequently the 70% change observed above (in 50 ms) could arise either as a consequence of a still finite population of native enzyme (N) following the establishment of the pseudo-equilibrium $I_3 \rightleftharpoons N$ or, alternatively, I_3 may possess some residual structure detected by tyrosine absorbance in the present unfolding conditions.

Discussion

(*a*) *The Loss of 2′CMP Binding Parallels the Exposure to Solvent of the Buried Tyrosine Groups.* At present, I_3 is the earliest known intermediate in the unfolding of RNase A. Characterization of its properties provides information about the first detectable step in unfolding. A question of basic interest is whether more than one stage in the refolding in I_3 can be observed, particularly when its refolding is monitored by different probes. Following the selective population of I_3 by a 50-ms period of unfolding (pH 5.8 → 2.0, 47 °C), a refolding jump (pH 2.0 → 5.8, 47 °C) is accompanied by the reappearance of the ability of RNase A to bind the inhibitor, 2′CMP (Table II). The kinetics of reappearance of inhibitor binding are nearly identical with those observed for reburying the tyrosines (λ = 287 nm). The loss of 2′CMP binding cannot be studied by an unfolding experiment alone since the association constant of RNase A for 2′CMP is drastically reduced at low pH and 2′CMP dissociation is rapid compared with the dead-time of the stopped flow. Under refolding conditions, reassociation of 2′CMP with native RNase A is very rapid (<3 ms; Hammes, 1968; cf. Garel & Baldwin, 1973) and, as a result, the finite time of reappearance of 2′CMP binding represents the formation of the binding site. The parallel reappearance of 2′CMP binding and formation of buried tyrosines in refolding from I_3 indicates that formation of the 2′CMP binding site does not precede measurably the exclusion of water from the buried tyrosine groups.

Moreover, the overall folding process, starting from the largely unfolded intermediate I_3, takes place in about 30 ms (see Table I), which is more rapid than had been supposed previously.

(*b*) *The Species (I_3) Is Distinct from Previously Described Intermediates in Refolding.* In their study of the effects of Gdn·HCl on the kinetics of refolding in RNase A, Nall et al. (1978) observed that, while the ratio of the amplitudes of the fast and slow phases in refolding was not affected by Gdn·HCl, there were striking changes in the rate and apparent $\Delta H^{\ddagger}$ of the $U_1 \rightleftharpoons U_2$ reaction produced by low concentrations of Gdn·HCl. On the basis of these results, Nall et al. (1978) suggested a possible model

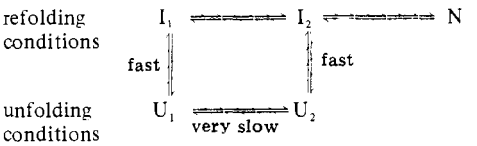

where the U ⇌ I interconversions are rapid compared with the $U_1 \rightleftharpoons U_2$ and $I_1 \rightleftharpoons I_2$ reactions. The species U_1 and U_2 are presumed to have lost essentially all of their secondary structure except as constrained by the presence of S–S bonds. The species I_1 and I_2 are postulated to have some partly folded structure which facilitates the interconversion between I_1 and I_2 and causes a reduction in the apparent $\Delta H^{\ddagger}$. Prior to the current study, no information existed relating the species (I_3) observed in unfolding experiments to these refolding intermediates (I_1 and I_2), or to the species U_1 and U_2. In the sequential unfolding/refolding experiment (pH 5.8 → 2.0 → 5.8, 47 °C), the $I_3 \rightarrow N$ reaction takes place on a much faster time scale than either $I_2 \rightarrow N$ or $I_1 \rightarrow N$ reactions (Table II). Therefore, the species (I_3) must be distinct from I_1 and I_2 (the same argument holds for U_1 and U_2) and cannot proceed through either I_1 or I_2 species in refolding. Similar measurements of the rate of $I_3 \rightarrow N$ conversion, monitoring binding of 2′CMP (A_{250}), yield essentially identical values for τ_3. Further support for the conclusion that I_1 and I_2 are not substantially populated during the 50-ms unfolding period is based on the absence of any significant kinetic complexity for refolding from I_3. The slight sloping base line of the amplitude curve (Figure 4) may reflect a slight amount of population of I_2 during the 50-ms delay.

In unfolding at pH 6.0, both T-jump experiments and stopped-flow experiments adding Gdn·HCl failed to demonstrate the presence of I_3 at this pH, even for unfolding jumps ending well above the final transition zone (Nall, 1976). Therefore, the species (I_3) must be pH dependent. Apart from this and the observation that I_3 is distinct from I_1, I_2, U_1, and U_2, nothing at present can be said concerning the relationship between the unfolding process

$$N \rightarrow I_3 \rightarrow U_2 \rightleftharpoons U_1$$

and the postulated refolding process (Nall et al., 1978).

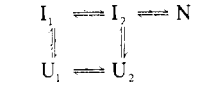

(c) *Sequential Unfolding/Refolding Experiments Provide a Powerful Means of Characterizing Transient Folding Intermediates.* Prior to the present study of the kinetics of folding of RNase A, little information existed concerning the pathway of interconversion between I_2 and N, except for the observation of a rapidly formed, transient intermediate (I_3) in unfolding (Hagerman & Baldwin, 1976). This intermediate is apparently never populated to an extent greater than 1–2% at equilibrium, and this would not be detected in refolding jumps starting from equilibrium conditions. In order to further characterize I_3, a sequential-mixing apparatus has been employed, thus allowing the initiation of a second reaction as early as 5 ms after the first reaction has been initiated. Such an experimental approach possesses the distinct advantage over conventional single process, stopped-flow experiments, in that transient intermediates can be selectively populated and their

subsequent behavior followed under conditions where these intermediates would not normally be populated to any significant degree.

Acknowledgments

We appreciate very much the help and advice of Dr. Will McClure in building the sequential mixing apparatus. We are indebted to Dr. Julian Sturtevant for the suggestion that DCIP be used to calibrate the instrument. Finally, we are grateful to the National Science Foundation for giving us the funds to build the apparatus.

References

Ballou, D. P. (1971) Ph.D. Dissertation, University of Michigan.

Beaven, G. H., Holiday, E. R., & Johnson, E. H. (1955) in *The Nucleic Acids* (Chargaff, E., & Davidson, J. N., Eds.) Vol. 1, p 513, Academic Press, New York.

Blum, A. D., Smallcombe, S. H., & Baldwin, R. L. (1978) *J. Mol. Biol. 118*, 305–316.

Garel, J.-R., & Baldwin, R. L. (1973) *Proc. Natl. Acad. Sci. U.S.A. 70*, 3347–3351.

Garel, J.-R., & Baldwin, R. L. (1975a) *J. Mol. Biol. 94*, 611–620.

Garel, J.-R., & Baldwin, R. L. (1975b) *J. Mol. Biol. 94*, 621–632.

Hagerman, P. J. (1977) Ph.D. Dissertation, Stanford University.

Hagerman, P. J., & Baldwin, R. L. (1976) *Biochemistry 15*, 1462–1473.

Hammes, G. G. (1968) *Adv. Protein Chem. 23*, 1–57.

Nall, B. T. (1976) Ph.D. Dissertation, Stanford University.

Nall, B. T., Garel, J.-R., & Baldwin, R. L. (1978) *J. Mol. Biol. 118*, 317–330.

Sela, M., & Anfinsen, C. B. (1957) *Biochim. Biophys. Acta 24*, 229–235.

Tonomura, B., Nakatani, H., Ohnishi, M., Yamaguchi-Ito, J., & Hiromi, K. (1978) *Anal. Biochem. 84*, 370–383.

Tsong, T. Y., Baldwin, R. L., & Elson, E. L. (1972) *Proc. Natl. Acad. Sci. U.S.A. 69*, 1809–1812.

Laser-Raman Investigation of Phospholipid–Polypeptide Interactions in Model Membranes†

Heino Susi,* Joseph Sampugna,‡ J. W. Hampson, and J. S. Ard

ABSTRACT: The interaction of aqueous dimyristoylphosphatidylcholine liposomes with the polypeptides gramicidin A, poly-L-lysine, valinomycin, and gramicidin S was investigated by means of laser-Raman spectroscopy. Auxiliary data were obtained with differential scanning calorimetry. Studies were carried out over the temperature range of 0–50 °C, encompassing the gel phase, the transition region, and the liquid crystalline phase of the liposomes. Conformational changes in the phospholipid molecules were investigated by measuring the intensity of the 1062-cm^{-1} Raman band which is assigned to C–C stretching vibrations of trans segments. Three different types of phospholipid–polypeptide interactions were indicated by the observed Raman data. They are interpreted as (a) orderly penetration of the phospholipid bilayer by a hydrophobic polypeptide; (b) polar interactions involving primarily the head groups of the phospholipid; and (c) disorderly hydrophobic binding between a polypeptide and the hydrocarbon domain of the phospholipid.

Raman spectroscopy has been shown to be an effective tool for structural studies of phospholipid molecules in natural as well as model membrane systems (Lippert & Peticolas, 1971; Larsson & Rand, 1973; Mendelsohn et al., 1975; Verma & Wallach, 1976; Yellin & Levin, 1977a–c). The sensitivity of several spectral features to conformational changes of the hydrocarbon chains provides a way to investigate the trans–gauche isomerism and, thus, the fluidity of bilayer assemblies (Lippert & Peticolas, 1971; Mendelsohn, 1972; Larsson & Rand, 1973; Gaber & Peticolas, 1977; Yellin & Levin, 1977a). 1,2-Diacylphosphatidylcholine–water bilayer systems are frequently accepted as models for the more complicated cellular membranes (Lippert & Peticolas, 1971; Mendelsohn, 1972; Mendelsohn et al., 1975; Gaber & Peticolas, 1977; Yellin & Levin, 1977c). The fluidity of model membranes in the gel phase as a functon of temperature has been investigated in some detail by Raman spectroscopy for systems composed of pure dimyristoyl, dipalmitoyl, and distearoyl phosphatidylcholine liposomes (Yellin & Levin, 1977a,b). Raman studies over a considerable temperature range have also been reported for the systems dipalmitoylphosphatidylcholine–cholesterol (Lippert & Peticolas, 1971) and dipalmitoylphosphatidylcholine–gramicidin A (Chapman et al., 1977; Weidekamm et al., 1977). Both cholesterol and gramicidin A increase the liposome fluidity in the gel phase and decrease it in the liquid crystalline phase. Several Raman studies showing phospholipid–polypeptide interactions have been carried out at room temperature or at a few selected temperature values (Larsson & Rand, 1973; Verma & Wallach, 1976; Lis et al., 1976a,b). Related studies have been conducted with differential scanning calorimetry (Chapman et al., 1977; Papahadjopoulos et al., 1975; Chapman et al., 1974).

The present communication is concerned with a laser-Raman study of the interactions of several different polypeptides with the bilayers of 1,2-dimyristoyl-L-phosphatidylcholine as a function of temperature. Dimyristoyl-

† From the Eastern Regional Research Center, Federal Research, Science and Education Administration, U.S. Department of Agriculture, Philadelphia, Pennsylvania 19118. *Received July 6, 1978.*

‡ Senior Sabbatical Fellow supported in part by the Dairy Research Foundation and the University of Maryland. Present address: Chemistry Department, University of Maryland, College Park, MD 20740.